ACS APPLIED MATERIALS & INTERFACES

Research Article

www.acsami.org

Structural Reorganization and Fibrinogen Adsorption Behaviors on the Polyrotaxane Surfaces Investigated by Sum Frequency Generation Spectroscopy

Aimin Ge,[†,§] Ji-Hun Seo,[‡] Lin Qiao,[†] Nobuhiko Yui,[‡] and Shen Ye*[,†]

[†]Catalysis Research Center, Hokkaido University, Sapporo 001-0021, Japan

[‡]Institute of Biomaterials and Bioengineering, Tokyo Medical and Dental University, Tokyo 101-0062, Japan

Supporting Information

ABSTRACT: Polyrotaxanes, such as supramolecular assemblies with methylated α-cyclodextrins (α-CDs) as host molecules noncovalently threaded on the linear polymer backbone, are promising materials for biomedical applications because they allow adsorbed proteins possessing a high surface flexibility as well as control of the cellular morphology and adhesion. To provide a general design principle for biomedical materials, we examined the surface reorganization behaviors and adsorption conformations of fibrinogen on the polyrotaxane surfaces with comparison to several random copolymers by sum frequency generation (SFG) vibrational spectroscopy. We showed that the polyrotaxane (OMe-PRX-PMB) with methylated α-CDs as the host molecule exhibited unique surface structures in an aqueous environment. The hydrophobic interaction between the methoxy groups of the methylated α-CD molecules and methyl groups of the *n*-butyl methacrylate (BMA) side chains may dominate the surface restructuring behavior of the OMe−PRX−PMB. The orientation analysis revealed that the orientation of the fibrinogen adsorbed on the OMe−PRX−PMB surface is close to a single distribution, which is different from the adsorption behaviors of fibrinogen on other polyrotaxane or random copolymer surfaces.

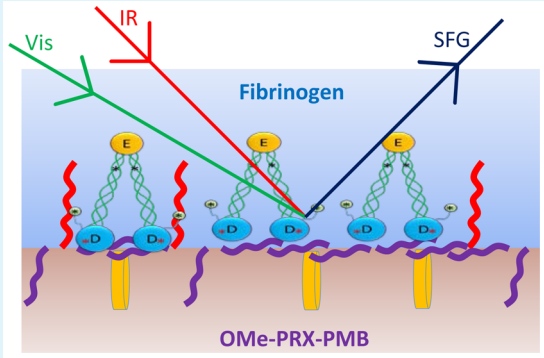

KEYWORDS: *biomedical materials, polyrotaxane, α-cyclodextrin (α-CD), surface reorganization, fibrinogen adsorption, SFG vibrational spectroscopy*

1. INTRODUCTION

Biocompatibility is one of the most important characteristics of a biomaterial whose surface directly interacts with a biological system.[1] It has been well demonstrated that the surface properties of the biomaterials play a critical role in determining the structure and conformation of adsorbed proteins, which significantly correlates with nonspecific biological activities such as blood clotting and inflammatory reactions.[1] For this reason, a series of polymeric materials with tailored surface properties have been synthesized and investigated for biomedical applications.[1,2] Recent advances have revealed that the surface flexibility of biomaterials can affect the biological responses, such as cellular morphology and adhesion.[3] In particular, polyrotaxanes, supramolecular assemblies in which guest molecules are noncovalently threaded by host molecules,[4,5] have become promising materials for biomedical applications because they allow reduction of nonspecific biological interactions and biocompatibility enhancement.

In our recent studies, we (N.Y.) have systematically investigated the biomedical application of polyrotaxanes for the regulation of protein adsorption and cell adhesion behaviors.[3,6−9] Figure 1 shows the molecular structures of two typical polyrotaxanes, PRX−PMB and OMe−PRX−PMB, which contain a guest molecule of a linear polyethylene glycol (PEG) and host molecules of α-cyclodextrin (α-CD) and methylated α-CD molecules.[3,6] Among these polyrotaxanes and random copolymers, the highest amounts of human fibrinogen with the highest flexibility were found to be adsorbed on the OMe−PRX−PMB surface. Human fibrinogen, which forms a blood clot in conjunction with platelets over a wound site, is known as a common blood protein with the molecular weight of 340 kDa.[10,11] It has been reported that the adsorbed fibrinogen can enhance the adsorption of platelets in the blood.[12,13] In our previous study, however, it was found that even though the amount of adsorbed fibrinogen on OMe−PRX−PMB was 5 times higher than those on the other polymers, a low level of platelet adhesion was observed.[6] This result indicates that the adsorption conformation of fibrinogen on the OMe−PRX−PMB surface should be different. Despite the promising biomedical performances, it is still unclear how the host molecules in the polyrotaxanes affect the surface

Received: August 20, 2015
Accepted: September 22, 2015
Published: September 22, 2015

DOI: 10.1021/acsami.5b07760
ACS Appl. Mater. Interfaces 2015, 7, 22709−22718

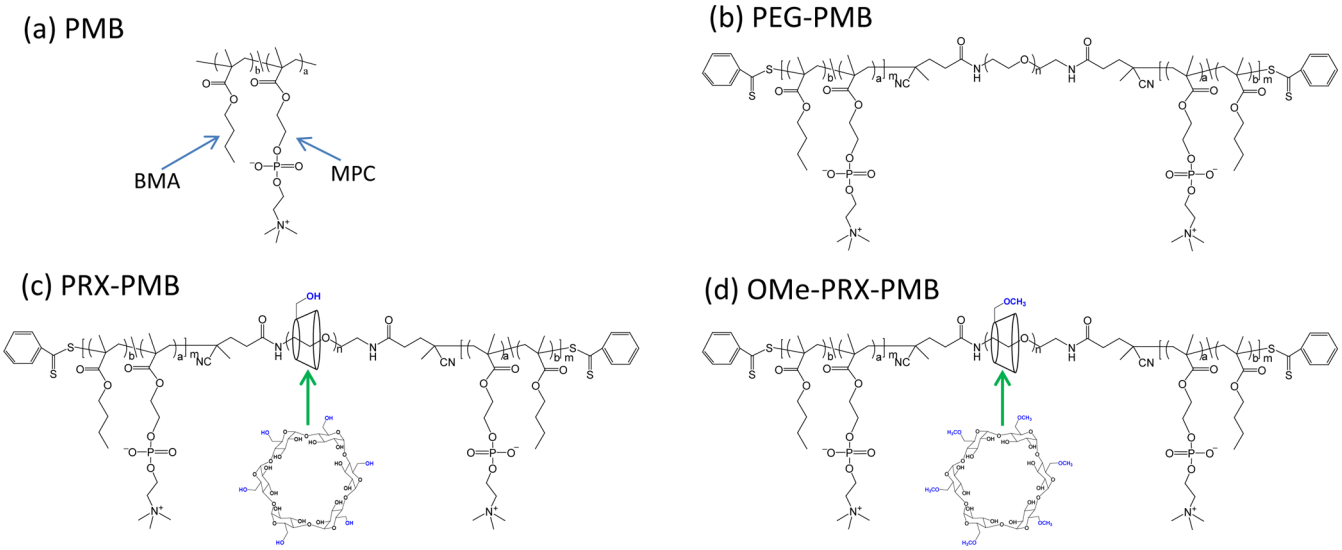

Figure 1. Molecular structures of random copolymers and polyrotaxanes, (a) poly((2-methacryloyloxyethyl phosphorylcholine)-*co*-(*n*-butyl-methacrylate)) (PMB), (b) PMB-polyethylene glycol (PEG−PMB), (c) PMB−PEG−polyrotaxane (PRX−PMB), and (d) PMB−PEG-methylated polyrotaxane (OMe−PRX−PMB). Only six methoxy groups are depicted in the molecular structure of methylated alpha-CD for clarity.

Table 1. Molecular Composition of Polymers Used in This Work

	BMA (mol % in PMB)	MPC (mol % in PMB)	BMA (wt %)	MPC (wt %)	no. of α-CD	methylation (%)	methoxy (wt %)
PMB	81	19	67	33	0		
PEG−PMB	77	23	48[c]	29[c]	0		
PRX−PMB[a,b]	88	12	53	15	12	0	
OMe−PRX−PMB[a,b]	88	12	53	15	12	>90	6.1

[a]Number-average molecular weight (Mn) of PRX−PMB and OMe−PRX−PMB, 99k. [b]PMB segment in PRX−PMB and OMe−PRX−PMB is 68 wt %. [c]The weight fractions of BMA and MPC in the PEG−PMB molecule are estimated by assuming the weight fractions of PMB and PEG in PEG−PMB are same as those in PRX−PMB and OMe−PRX−PMB.

properties and then the fibrinogen adsorption behaviors on the polymer surface.

Sum frequency generation (SFG) spectroscopy, a second-order nonlinear vibrational spectroscopic technique, has emerged as a powerful tool for the characterization of polymer interfaces in the past decade.[14−17] Because only noncentrosymmetric media is SFG-active, SFG offers insights into the molecular structures at the polymer interfaces where inversion symmetry is broken.[18] SFG has several advantages in comparison to other common surface-sensitive vibrational spectroscopies. For instance, it does not require rough metal substrates which are necessary for surface-enhanced Raman scattering. So far, the SFG vibrational spectroscopy has been applied to elucidate the surface restructuring,[19−24] molecular orientation,[25] ordering transition,[26] protein adsorption,[27−29] and hydrogen bonding at polymer interfaces.[30]

In this study, the SFG spectroscopy was employed to investigate the effect of host molecules on the structural reorganization of polyrotaxanes in an aqueous environment. The random copolymers (PMB and PEG−PMB, Figure 1a,b) and polyrotaxanes (PRX−PMB and OMe−PRX−PMB, Figure 1c,d) offer a unique opportunity to investigate the effect of host molecules on the surface structure of polyrotaxanes. We observed that the interfacial structures of these polymers mostly depend on the environment. All of these polymers show similar side chain structures at the interface with air, but only the polyrotaxane with methylated α-CDs (OMe−PRX−PMB, Figure 1d) shows some ordered interfacial structures at the interface with water. On the basis of the comparison of the surface structure differences between PRX−PMB and OMe−PRX−PMB, we believed that the methylated α-CDs facilitate the surface reorganization of the polyrotaxane in the aqueous environment. It is believed that the ordered structures at the OMe−PRX−PMB/water interface can be attributed to the hydrophobic interaction between the methoxy groups of the methylated α-CD molecules and methyl groups of the *n*-butyl methacrylate (BMA) side chains. Furthermore, SFG spectroscopy was used to investigate the fibrinogen adsorption conformation on these polymer surfaces. The present study revealed that the fibrinogen molecules adsorbed on the OMe−PRX−PMB surface have different conformations in comparison to those on other polymer surfaces.

2. EXPERIMENTAL SECTION

Materials. The details about the synthetic process of the random copolymers and polyrotaxanes have already been described elsewhere.[3,6] Figure 1 shows the chemical structures of the polymers investigated in the study, i.e., poly((2-methacryloyloxyethyl phosphorylcholine)-*co*-(*n*-butyl- methacrylate)) (PMB), PMB-polyethylene glycol (PEG−PMB), PMB−PEG−polyrotaxane (PRX−PMB), and PMB−PEG-methylated polyrotaxane (OMe−PRX−PMB). PMB contains two kinds of side chains, a relatively hydrophilic 2-methacryloyloxyethyl phosphorylcholine (MPC) and relatively hydrophobic *n*-butyl methacrylate (BMA). PMB−polyethylene glycol (PEG−PMB) consists of two PMB segments connected to the terminals of a polyethylene glycol (PEG) backbone (Figure 1b). PRX−PMB and OMe−PRX−PMB are assembled by threading 12 α-CDs and 12 methylated α-CDs (methylation degree >90% for the 18 OH groups on the outside of α-CDs) per linear polyethylene glycol,

DOI: 10.1021/acsami.5b07760
ACS Appl. Mater. Interfaces 2015, 7, 22709−22718

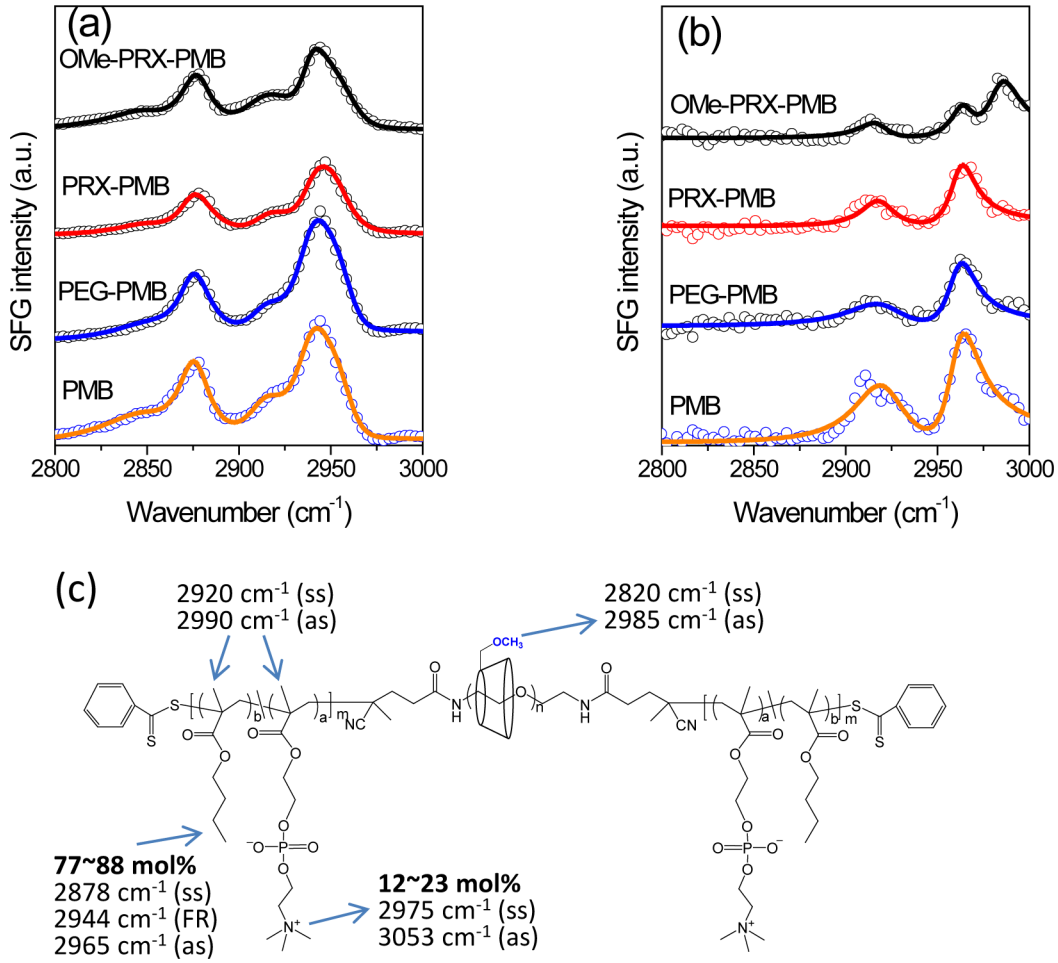

Figure 2. (a) *ssp*-polarized and (b) *sps*-polarized SFG spectra in the C−H stretching region for polymer/air interfaces. (c) Possible peak positions of CH_3, α-CH_3, N−CH_3, and OCH_3 groups. Open cycles represent experimental data. Solid lines represent fitting results. The scales in parts a and b are offset for clarity.

respectively (Figure 1c,d). The PMB was anchored to the terminals of the polyethylene glycol backbone as a stopper to form a polyrotaxane molecule. The threaded α-CDs of PRX−PMB and methylated α-CDs of OMe−PRX−PMB only occupy approximately 5−8% of the space of the polyethylene glycol backbone based on the estimation of their geometric sizes, thus α-CDs or methylated α-CDs have enough space to move if they can. The molecular composition of polymers used in this study is given in Table 1.

The phosphate buffered saline (PBS, $CaCl_2$ (−), $MgCl_2$ (−), pH 7.4) was purchased from GIBCO. Human plasma fibrinogen (F4129, powder) was purchased from Sigma. Pure water (Milli-Q, resistivity >18.2 MΩ cm) was used. Heavy water (99.90% D) was purchased from Eurisotop. All chemicals were used as received without further purification.

Sample Preparation. The stock solutions of the polymers were prepared at a concentration of 0.5 mg/mL in mixture of CH_3OH−H_2O (1:1 in volume).[6] The polymer thin-films with a thickness of about 20 nm were prepared by casting 100 μL of the polymer solution on the flat surface of a CaF_2 hemicylindrical prism (2.5 × 2.5 cm^2). The films were dried on a clean bench for 24 h before the SFG characterizations at the polymer/air interface. For the SFG measurement in aqueous solutions, the dried samples were immersed in pure water for 24 h to stabilize the film structures in the water. A homemade Teflon cell (volume 2 mL) was used for the SFG characterization at the polymer/water interface by filling the cell with pure water. In the protein adsorption experiments, the fibrinogen solution with a concentration of 0.3 mg/mL in PBS was injected into the Teflon cell and allowed to contact the polymer films for 30 min before the SFG measurement. No change in the SFG spectra was observed for a longer immersion period. After replacing the fibrinogen solution by the buffer solution, similar SFG spectra were observed, indicating that the SFG signals of the fibrinogen in the spectra were essentially due to the adsorbed molecules at the interface rather than the molecules in the bulk solution.

SFG Measurement. The SFG system has been described in detail elsewhere.[31−33] Briefly, a 1 kHz, 2 W Ti:sapphire regenerative amplifier produces 120 fs pulses at 800 nm. Half of the amplifier's output is directed into an optical parametric amplifier (OPA) followed by difference frequency generation (DFG) to generate the mid-IR pulses. The IR pulses are tunable from 2.5 to 10 μm with a spectral width of ~200 cm^{-1}. The other half of the amplifier's output is directed into a homemade pulse shaper to generate ~10 ps pulses with a spectral width of ~10 cm^{-1}. The SFG signal was recorded by a CCD detector (DU420-BV, Andor Technology) attached to a spectrograph (MS3504, Solar-TII, f = 35 cm, 1200 grooves/mm for the visible region or 600 grooves/mm for the UV region).

The total internal reflection mode (near total internal reflection for the polymer/liquid interface) was adopted in all SFG measurements. The angles of incidence were 50° and 70° for the IR and visible beams, respectively. The *ssp* and *sps* polarization combinations of SFG, visible, and infrared beams were used for the polymer interfaces. *ppp* and *ssp* polarization combinations were used for polymer/fibrinogen solution interfaces. A purge of dry air into the measurement box was required for measurements in the C═O and O−H stretching regions to avoid the influence of water molecules in the air. The SFG spectra of the samples were normalized by the SFG spectra of a gold thin film evaporated on a CaF_2 hemicylindrical prism.

DOI: 10.1021/acsami.5b07760
ACS Appl. Mater. Interfaces 2015, 7, 22709−22718

Orientation Analysis. The SFG spectra can be fitted using the following equation:[34−37]

$$I \propto |\chi_{\mathrm{R}}^{(2)} + \chi_{\mathrm{NR}}^{(2)}|^2 = \left| N \sum_n \frac{A_n}{\omega_{\mathrm{IR}} - \omega_{v,n} + i\Gamma_n} + \chi_{\mathrm{NR}}^{(2)} \right|^2 \quad (1)$$

where I is the SFG intensity. $\chi_{\mathrm{R}}^{(2)}$ and $\chi_{\mathrm{NR}}^{(2)}$ are the resonant and nonresonant nonlinear susceptibilities, respectively. N is the molecular density on the surface. A_n, $\omega_{v,n}$, and Γ_n are the amplitude, resonant frequency, and damping coefficient of the nth vibrational mode, respectively. In the present study, we have analyzed the orientation of the BMA side chains at the polymer/air interfaces and the fibrinogen molecules adsorbed at the polymer/fibrinogen solution interfaces. The orientation analysis method of BMA side chains is briefly described as follows.

The effective nonlinear susceptibilities under the *ssp*- and *sps*-polarization combinations can be expressed as[38]

$$\chi_{\mathrm{eff},ssp}^{(2)} = L_{yy}(\omega_{\mathrm{SF}})L_{yy}(\omega_{\mathrm{Vis}})L_{zz}(\omega_{\mathrm{IR}}) \sin\theta_{\mathrm{IR}}\chi_{yyz}^{(2)} = L_{yyz}\chi_{yyz}^{(2)} \quad (2)$$

$$\chi_{\mathrm{eff},sps}^{(2)} = L_{yy}(\omega_{\mathrm{SF}})L_{zz}(\omega_{\mathrm{Vis}})L_{yy}(\omega_{\mathrm{IR}}) \sin\theta_{\mathrm{Vis}}\chi_{yzy}^{(2)} = L_{yzy}\chi_{yzy}^{(2)} \quad (3)$$

where L_{yyz} and L_{yzy} are the Fresnel coefficients determined by the experimental geometry and the refractive index of the mediums, respectively.[38] In the present study, the values of L_{yyz} and L_{yzy} are 3.06 and 2.55, respectively. $\chi_{yyz}^{(2)}$ and $\chi_{yzy}^{(2)}$ for the asymmetric C−H stretching mode of the methyl group can be written as follows:[39]

$$\chi_{yyz,\mathrm{as}}^{(2)} = -N\beta_{caa}(\cos\theta - \cos^3\theta) \quad (4)$$

$$\chi_{yzy,\mathrm{as}}^{(2)} = N\beta_{caa}\cos^3\theta \quad (5)$$

where θ is the orientation angle of the methyl group and defined as the angle between the surface normal and the symmetric axis of the methyl group. β_{caa} is the hyperpolarizability of the methyl group. The operator $\langle\ \rangle$ is employed to carry out an ensemble average of the orientation angle by the distribution function $f(\theta)$. On the basis of eqs 4 and 5, we can find that the ratio of $\chi_{yyz,\mathrm{as}}^{(2)}/\chi_{yzy,\mathrm{as}}^{(2)}$ is only dependent on the orientation angle θ. Because the values of $\chi_{yyz,\mathrm{as}}^{(2)}$ and $\chi_{yzy,\mathrm{as}}^{(2)}$ can be, respectively, obtained from the *ssp*- and *sps*-polarized SFG spectra, the orientation angle θ can be calculated. If the hydrocarbon chains are in the all-trans conformation, the tilt angle (α) with respect to the surface normal of the chain can be induced by $\alpha = |35.2° - \theta|$.[34,35,38,40]

3. RESULTS AND DISCUSSION

Molecular Structures at the Polymer/Air Interface. Figure 2a shows the *ssp*-polarized SFG spectra (circles) in the C−H stretching region (2800−3000 cm^{-1}) observed on the surface of various polymers in air. The fitting results based on eq 1 are also given in the same figure (solid traces, Figure 2a). The SFG spectra are dominated by two strong peaks at 2878 and 2944 cm^{-1}, which can be assigned to the CH_3 symmetric stretching ($CH_{3,ss}$) and the Fermi resonance ($CH_{3,FR}$) between $CH_{3,ss}$ and the overtone of the C−H bending, respectively. Weak peaks at 2850 and 2915 cm^{-1} are also observed, which can be assigned to the CH_2 symmetric ($CH_{2,ss}$) and asymmetric ($CH_{2,as}$) stretching modes.[34,35] These *ssp*-polarized SFG spectra have similar spectral shapes, while the peak intensities slightly decrease in the sequence of PMB, PEG−PMB, PRX−PMB, and OMe−PRX−PMB.

Figure 2b shows the *sps*-polarized SFG spectra for these polymers under similar conditions. All the samples show two peaks at 2915 and 2965 cm^{-1}. These peaks can be assigned to $CH_{2,as}$ and $CH_{3,as}$, respectively. An additional peak at 2985 cm^{-1} was only observed for OMe−PRX−PMB, which is assigned to the OCH_3 asymmetric stretching mode. This indicates that the methylated α-CDs moieties on the OMe−PRX−PMB surface have a certain ordering.[41] Similar to the *ssp* spectra, a decrease in the peak intensities was also observed in the sequence of PMB, PEG−PMB, PRX−PMB, and OMe−PRX−PMB, which should be attributed to the decrease in the surface density of the BMA side chains after adding PEG and α-CDs on the polymers.

In comparison to the possible C−H vibrational modes in the OME (Figure 2c), we assigned the SFG peaks observed in our *ssp*- and *sps*-polarized SFG spectra (Figure 2a,b) to those of the terminal methyl groups on the BMA side chains. On the basis of the calculation methods described by eqs 2−5, we are able to estimate the orientation angles of the BMA side chains on these polymer surfaces (Table 2). The calculation reveals that the BMA side chains have similar tilt angles on these polymer surfaces. These results indicate that the polymer surfaces in air are mainly covered by the BMA side chains. Although the BMA side chains account for 77−88 mol % of the side chains or 48−53 wt % of the whole molecules (Figure 1 and Table 1), this may not be the only reason for this specific surface enrichment. The hydrophobic BMA side chains in these polymers tend to stand up in air in comparison to the MPC side chains with a zwitterionic choline group. Generally, as the polymers become exposed to air, the hydrophobic segments are expected to cover most of the polymer surface in the air, while the hydrophilic side chains will orient toward the polymer bulk to minimize the interfacial free energy.[19,20] It is reasonable that the polymer surfaces are mainly covered by the hydrophobic BMA side chains, while the zwitterionic MPC chains prefer being toward the bulk of the polymer thin films. In the case of OMe−PRX−PMB, the SFG peak of the methylated α-CDs was observed (Figure 2b) in addition to the spectral features of BMA side chains. This indicates that both methylated α-CDs and BMA side chains are present on the OMe−PRX−PMB surface. For PRX−PMB, however, there is no direct spectral evidence of whether the α-CDs are present at the PRX−PMB/air interface because they have no C−H stretching peak in the SFG spectrum.

Table 2. Orientation Angle of Methyl Group in BMA Chains and Tilt Angle of BMA Chains Assuming a δ-Distribution[a]

sample	tilt angle of methyl on BMA (θ)	tilt angle of BMA chain (α)
PMB	51°	16°
PEG−PMB	54°	19°
PRX−PMB	57°	22°
OMe−PRX−PMB	61°	26°

[a]The angles were calculated on the basis of fitting results of SFG spectra with ±5° error.

SFG measurements were also carried out in the C═O stretching region for the carbonyl groups of these polymers (Figure 3). All the polymers showed two peaks at 1735 and 1715 cm^{-1} except for OMe−PRX−PMB, which exhibits a single and broad peak around 1715 cm^{-1}. These peaks are apparently assigned to the C═O stretching mode of the carbonyl groups in the polymers. On the basis of the previous discussion about the C−H stretching modes, most of the carbonyl groups should be those in the BMA side chains. The peak at 1735 cm^{-1} is assigned to the C═O stretching in the carbonyl groups of the BMA side chains, while that at the lower frequency (1715 cm^{-1}) is attributed as the C═O stretching of

DOI: 10.1021/acsami.5b07760
ACS Appl. Mater. Interfaces 2015, 7, 22709−22718

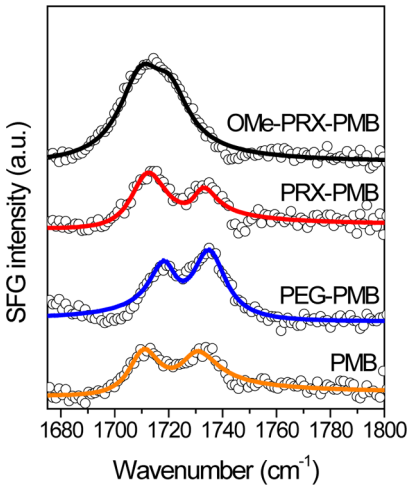

Figure 3. *ssp*-polarized SFG spectra in the C═O stretching region for polymer/air interfaces.

the hydrogen bonded carbonyl groups with a hydrogen bonding donor, such as water. It is known that the hydrogen bonding can shift the frequency of the C═O stretching to a lower frequency.[30] For OMe−PRX−PMB, the C═O stretching mode is dominated by a broad peak centered at 1715 cm^{-1}, indicating that the carbonyl groups tend to be hydrogen-bonded, possibly due to more water molecules remaining at the OMe−PRX−PMB/air interface. According to the present SFG observations, the methylated α-CDs at the OMe−PRX−PMB/air interface may play a role in keeping water molecules on the polymer surface. The hydrophobic interaction between methylated α-CDs and BMA side chains may further enhance the hydrogen bonding interaction between water molecules and C═O moieties.

Water-Induced Surface Reorganization of Polyrotaxanes. To understand the interfacial behaviors of these polymers in an aqueous environment, we investigated the surface structure of these polymers after immersion in water. Figure 4a shows the *ssp*-polarized SFG spectra in the C−H and O−H stretching region (2800−3700 cm^{-1}) of the polymers in contact with water. PMB, PEG−PMB, and PRX−PMB show several broad peaks in the O−H stretching region (3000−3700 cm^{-1}) while nothing in the C−H stretching region (2800−3000 cm^{-1}). The loss of the C−H signals from these polymers indicates that the ordered structures of the BMA side chains at the polymer/air interfaces (Figure 2a) were lost after immersion in the water. On the other hand, OMe−PRX−PMB exhibited two clear peaks around 2895 and 2960 cm^{-1} in the C−H stretching region as well as intense peaks in the O−H stretching region (Figure 4a). To further confirm the spectral feature of the OMe−PRX−PMB in the C−H stretching region, the SFG measurements were carried out in contact with the H_2O−D_2O mixture (1:2 in volume) instead of pure water. By this way, O−H peaks are significantly weakened due to inhibition of the Fermi resonances of the O−H modes by using heavy water. Thus, one can get an SFG peak in the C−H stretching region with less spectral interferences from the O−H peaks. As shown in Figure 4b,c, two C−H bands are clearly visible on the OMe−PRX−PMB interface while still nothing is observed on the PRX−PMB interface. The two C−H peaks of the OMe−PRX−PMB/water interface are intensified in Figure 4a due to the interference with the SFG signals in the O−H stretching region based on the general principle of SFG (see, for example, eq 1). Although the peak intensities in the H_2O−D_2O mixture are much weaker than those of the OMe−PRX−PMB/air interface (Figure 4b), the presence of C−H stretching signals arising from the OMe−PRX−PMB segments suggests that there are some ordered surface structures on the OMe−PRX−PMB surface in the aqueous solution.

Although these two peaks on the OMe−PRX-PMB surface in air and in water seem to be alike, they are clearly different in peak positions, indicating that the original peaks on the OMe−PRX-PMB/air interface disappeared and novel peaks appeared in water. The peak at 2960 cm^{-1} is assigned to the $CH_{3,as}$ of the terminal methyl group of the BMA side chains. The peak at 2895 cm^{-1} observed in the H_2O−D_2O mixture seems to be much wider and contains a contribution from both the $CH_{3,ss}$ and $CH_{2,as}$ modes of the BMA side chains. As shown in Figure 4b, the *ssp*-polarized spectrum of OMe−PRX−PMB in water is dominated by the CH_3as peak. This is very different from that of OMe−PRX−PMB in air, suggesting the terminal methyl group of the BMA chains tilt more toward the OMe−PRX−PMB surface in water.[22]

The surface ordering of OMe−PRX−PMB in water is further supported by our SFG observation of the C═O stretch peak at 1715 cm^{-1} at the OMe−PRX−PMB/water interface (Figure 5).

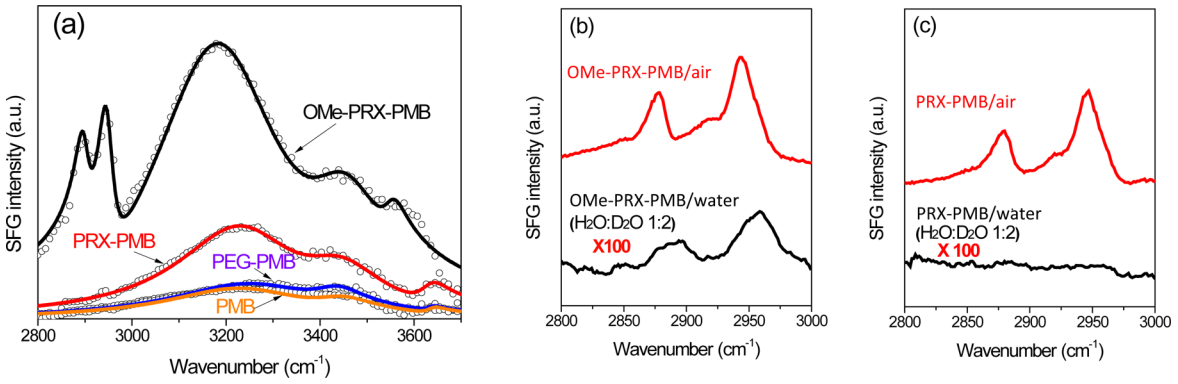

Figure 4. (a) *ssp*-polarized SFG spectra in the C−H and O−H stretching regions of polymer/water interfaces. The SFG spectrum of OMe−PRX−PMB shows strong bands in OH stretch region. Open symbols represent experimental data. Solid lines represent fitting results. Comparisons between *ssp* polarized SFG spectra in the C−H stretching region for polymer thin films in air (reproduced from Figure 2a) and in contact with the mixure of H_2O−D_2O (1:2 in volume), (b) OMe−PRX-PMB and (c) PRXPMB. The scales in parts b and c are offset for clarity. The data for polymer in contact with the mixure of H_2O:D_2O are smoothed for clarity.

DOI: 10.1021/acsami.5b07760
ACS Appl. Mater. Interfaces 2015, 7, 22709−22718

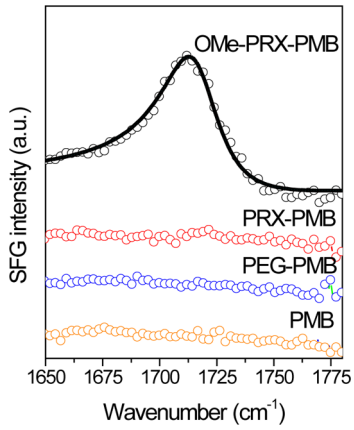

Figure 5. *ssp*-polarized SFG spectra in the C═O stretching region of polymer/water interfaces. Open symbols represent experimental data. Solid lines represent fitting results. The scale is offset for clarity.

No C═O stretching peak is observed for the other polymers, PRX−PMB, PEG−PMB, and PMB, in contact with water. Although OMe−PRX−PMB and PRX−PMB only differ in the termination state of the α-CDs (Figure 1c,d), their surfaces show totally different interfacial structures in water. On the other hand, we also found that the C−H and C═O signals of these polymers can be recovered again by drying the samples in the air, indicating the reversibility of the surface structures between air and water environments. This reversibility suggests that the structural changes in the polymers are mainly due to the reorientation of the side chains rather than the polymer backbone.

As already mentioned, the water structures on the polymer surfaces exhibit distinct features. Generally, the broad band between 3000 and 3500 cm^{-1} is attributed to the O−H stretch of the hydrogen-bonded water molecules. The strongest hydrogen-bonded O−H signals observed at the OMe−PRX−PMB/water interface indicate that the water molecules at the interface have a more ordered alignment among the four samples. In addition, PMB, PEG−PMB, and PRX−PMB show weak peaks at 3650 cm^{-1} which should be due to the free OH group of the water molecules near the hydrophobic polymer backbone or the hydrophobic side chains.[42−44] However, the free OH signal shifts to 3600 cm^{-1} for the OMe−PRX−PMB/water interface (Figure 4a). Again, not only the peak intensities but also the peak positions of the free OH band of the OMe−PRX−PMB/water interface are very different from those of the PRX−PMB/water interface.

To understand the interfacial behaviors of these polymers in water, we first considered the PMB, which has the simplest structure among the four polymers. At the polymer/water interface, it has also been reported that the hydrophilic side chains tend to orient toward water, while the hydrophobic part orients toward the bulk to minimize the surface energy.[20] On the PMB/water interface, we believe that the MPC side chains, which have hydrophilic phosphorylcholine groups, will reorient toward the water, while the hydrophobic BMA chains tend to reorient toward the polymer bulk. As a result, the SFG signals from the BMA chains were lost after contact with the water. The previous studies on the poly(*n*-butyl methacrylate) (PBMA), which also contains the BMA side chains, reported that the SFG signals arising from the BMA side chains are visible in water and the ordering of the polymer surface becomes even better.[22] The comparison between PMB and PBMA demonstrates that the MPC side chains in PMB can compete with the BMA chains to dominate the surface coverage of the PMB/water interface. Although the MPC chains may have a certain ordering on the surface, no C═O stretching signals from their ester groups were observed in the present study. This is possibly due to its low surface density (Table 1). In previous reports, the surface restructuring of the PMB in water, which results in the increased directionality of the hydrophilic MPC chains, has been used to explain the contact angle hysteresis (~40°) between the air and water.[6,45]

Previous studies about PEG−PMB showed that the swelling of the hydrophilic PEG may lead to a slight increase in the contact angle hysteresis in addition to the reorientation effect of the PMB segments.[6] Moreover, the hydrated loop-type PEG segment in the middle of the block copolymer was found to increase the molecular mobility.[6] In the present study, no apparent spectral differences between PEG−PMB and PMB

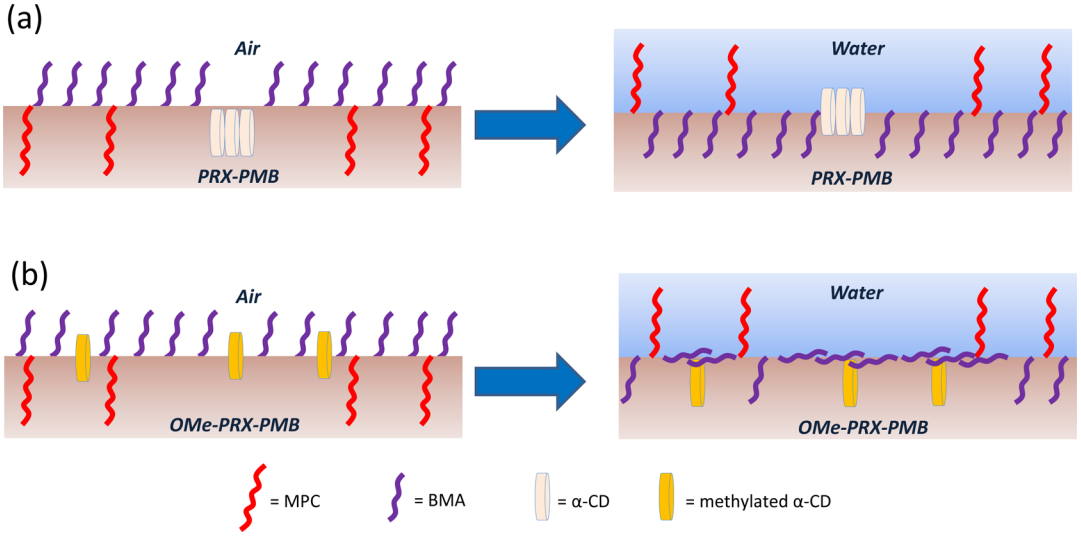

Figure 6. Schematic illustration of water induced surface restructuring at the (a) PRX-PMB/water and (b) OMe−PRX−PMB/water interfaces. The polymer backbone and water molecules are not depicted.

DOI: 10.1021/acsami.5b07760
ACS Appl. Mater. Interfaces 2015, 7, 22709−22718

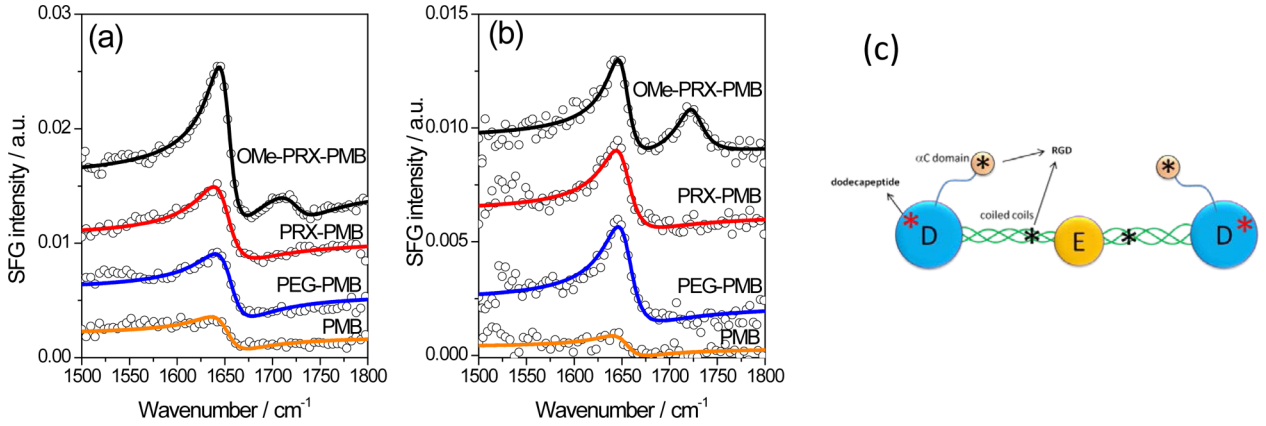

Figure 7. (a) *ppp*-polarized and (b) *ssp*-polarized SFG spectra of fibrinogen adsorbed on polymer surfaces. The SFG spectra were measured at polymer/fibrinogen solution interfaces. The solid lines are fitting results. The spectra are offset for clarity. (c) Structure of fibrinogen molecule. Binding sites for GPIIb/IIIa receptor of platelets are labeled with stars. RGD is abbreviation for arginine-glycine-aspartic acid; dodecapeptide is a peptide with 12 amino acids.

were observed. This indicates that the restructuring of the PMB segments in PEG−PMB should not be influenced by the presence of the PEG segment. Furthermore, since the PEG−PMB/water interface shows very similar O−H stretching modes as those of the PMB/water interface (Figure 4a), it is believed that the water molecules adsorbed on the PEG segment have an alignment similar as those on the PMB segment.

In the case of PRX−PMB, the hydrogen-bonded O−H stretching intensities of the water molecules adsorbed on the polymer surface were found to be higher than those of PEG−PMB (Figure 4a). This suggests that the presence of α-CD molecules threading on the PEG leads to an increased ordering of water alignment at the PRX−PMB/water interface. Previously, quartz crystal microbalance with dissipation (QCM-D) measurements revealed that the PRX−PMB surface has a lower surface mobility factor in comparison to PEG−PMB due to the rigid crystalline formation of the α-CD molecules by intermolecular hydrogen bonding.[6] On the basis of the present study, it is possible that the hydrogen bonding is not only formed among the α-CD molecules but also between α-CD and the water molecules. Since the PRX−PMB shows similar SFG signals as PEG−PMB in both the C−H and C═O stretching regions, there is no apparent evidence of interaction between the α-CD molecules and PMB segment in water. This can be possibly explained by the aggregation of the α-CD molecules due to intermolecular hydrogen bonding which reduces their influences on the PMB segment (Figure 6a).

We now discuss the surface reorganization of OMe−PRX−PMB in water. In previous studies, the OMe−PRX−PMB was found to show the highest surface mobility as well as the highest contact angle hysteresis among the four polymers.[6] To analyze the effect of the methylated α-CD molecules on the interfacial behaviors of polyroataxane in water, we focused on the comparison between OMe−PRX−PMB and PRX−PMB. As more than 90% of the hydroxyl groups on the exterior of the α-CD molecule is replaced by methoxy groups, the intermolecular hydrogen bonding between the α-CD molecules is expected to be dramatically decreased. The noncovalently threaded methylated α-CD molecules on the OMe−PRX-PMB are expected to have a much higher mobility than the hydroxylated α-CD molecules on the PRX−PMB. Although the current SFG measurement, which only provides temporally and spatially averaged structural information on the interface, cannot provide direct evidence of the surface mobility of the methylated α-CD molecules; the observed SFG signals from the BMA side chains and water molecules may correlate with such a special surface property for OMe−PRX−PMB. By comparing the SFG results observed on the PRX−PMB and OMe−PRX−PMB, we proposed that the hydrophobic interaction between the BMA chains and methylated α-CDs may be formed to get certain ordered structure of BMA chains at the OMe−PRX−PMB/water interface. As schematically illustrated in Figure 6b, as the OMe−PRX−PMB is in contact with water, the methylated α-CDs may tend to stay in the bulk or near the surface to minimize the surface energy. The hydrophobic interaction between the exterior of the methylated α-CDs and the BMA side chains may somewhat prevent part of the BMA chains from orienting toward the polymer bulk. We also believe that the aggregation of the methylated α-CDs should decrease the probability of such hydrophobic interaction. In other words, the dispersed state of the methylated α-CDs due to the high mobility may be beneficial to maximize the number of the of the BMA chains interacting with the methylated α-CDs. On the other hand, such a hydrophobic interaction is not expected or much weaker between the hydroxylated α-CDs and BMA chains at the PRX−PMB/water interface.

At the OMe−PRX−PMB/water interface, the C═O groups on the BMA side chains are believed to be oriented toward the water with a certain degree of ordering, producing the SFG signal in the C═O stretching region (Figure 5). On the other hand, the BMA chains orient toward the bulk which results in no C═O stretching signal at the PRX−PMB/water interface. Furthermore, the C═O stretching peak centered at 1715 cm^{-1} on the OMe−PRX−PMB surface indicates that the C═O groups are strongly hydrogen-bonded with water molecules (Figure 5). These hydrogen-bonded water molecules are expected to be well aligned and result in the strong hydrogen-bonded O−H stretch bands (Figure 4). As already discussed, we believe there are some ordered structures formed by the interaction between BMA and methylated α-CDs at the OMe−PRX−PMB/water interface. The frequency shift of the free O−H signal at the OMe−PRX−PMB/water interface may be attributed to the slight hydrogen-bonding of water molecules confined between the BMA and methylated α-CD moieties.

DOI: 10.1021/acsami.5b07760
ACS Appl. Mater. Interfaces 2015, 7, 22709−22718

Fibrinogen Adsorption on Polymer Surfaces. Fibrinogen consists of two symmetric parts, each part includes three different polypeptide chains labeled Aα, Bβ, and γ.[10,46] As shown in Figure 7c, the structure of the fibrinogen molecule can be separated by two D domains, one E domain, and two αC domains.[47,48] The D and E domains are connected by coiled-coils, while the D and αC domains are connected by αC chains. For each half of the fibrinogen molecule, there are three recognition sites for the integrin receptor GPIIb/IIIa of the platelets.[10] One is the dodecapeptide sequence close to the C-terminus of the γ-chain (γ400−411); the other binding sites are two RGD sequences on the α-chain (Aα572−574 and Aα95−97).[10] The positions of these binding sites on the fibrinogen molecule are described as stars in Figure 7c. Previous research revealed that the γ400−411 sites are strongly correlated with the adhesion of the platelets, while the relation between the RGD sites and platelets is not very clear.[12,13]

Figure 7 shows the (a) *ppp*- and (b) *ssp*-polarized SFG spectra in the C═O stretching region collected after fibrinogen adsorption on the PMB, PEG−PMB, PRX−PMB, and OMe−PRX−PMB surfaces. All the SFG spectra are dominated by a peak at 1650 cm^{-1}. It is noted that there are only two amide groups on each polymer main chain for PEG−PMB, PRX−PMB, and OMe−PRX−PMB (Figure 1). The control experiments on the polymer/PBS interfaces showed that no peak was observed around 1650 cm^{-1} in pure PBS (Figure S1b). Therefore, the peak at 1650 cm^{-1} in Figure 7 can be attributed to the fibrinogen adsorbed on the polymer surfaces. According to previous studies, this mode should arise from the amide I band of the α-helices of fibrinogen.[47,49,50] The signal should be attributed to the coiled-coils between the D and E domains (Figure 7c). The SFG signals from the β-sheet and random coils, usually at different peak positions, are not apparent in the present observations. The C═O stretching peak on the OMe−PRX−PMB surface is also observed, indicating the polymer surface structure is stable and not significantly changed after the fibrinogen adsorption. In addition, the two C−H stretching bands observed at the OMe−PRX−PMB/water interface also remain after the fibrinogen adsorption as shown in Figure S3.

In the present study, the amplitude ratio of the 1650 cm^{-1} peak between the *ppp*- and *ssp*-polarized SFG spectra is calculated as a dependence of the orientation angle based on the model proposed by Wang et al. (see the Supporting Information for details).[47] In this model, two coiled-coils of adsorbed fibrinogen are assumed to adopt the same orientation angle which is defined as the angle between the coiled-coils and surface normal. It is found that the amplitude ratios for PMB, PEG−PMB, and PRX−PMB cannot be explained by using either a single δ distribution or a single Gaussian distribution for the orientation angle as shown in Figure 8 (a schematic illustration of possible orientations of fibrinogen is shown in Figure S4). It is possible that the orientation angle has multiple distributions. Wang et al. previously reported that the adsorbed fibrinogen on a polystyrene surface can possibly have dual distributions for the two coiled-coils on the basis of SFG and polarized ATR-FTIR measurements.[47] On the other hand, the amplitude ratio for the fibrinogen on the OMe−PRX-PMB surface can be explained by a single orientation distribution. It has been reported that the fibrinogen adsorption is strongly affected by the hydrophobic interaction between the hydrophobic domains of fibrinogen and the surface.[51,52] The differences of the orientation distribution between fibrinogen on OMe−PRX−PMB surface and those on the other polymer surfaces should be attributed to the difference in the hydrophobic interaction between fibrinogen and polymers, especially when the methylated α-CD moieties are present.

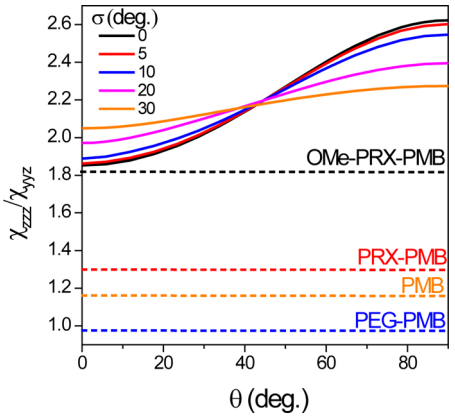

Figure 8. Relation between χ_{zzz}/χ_{yyz} ratio and orientation angle of fibrinogen. The χ_{zzz}/χ_{yyz} ratios for fibrinogen adsorbed on different polymer surfaces are described in the figure.

Even if a precise orientation determination for the adsorbed fibrinogen is still lacking due to its complicated structure, the present results clearly show that the adsorbed fibrinogen on OMe−PRX−PMB has a different conformation in comparison to those on the other polymer surfaces. A previous study revealed that the OMe−PRX−PMB surface shows a similar level of platelet adhesion even if there is a larger amount of adsorbed fibrinogen, which is possibly due to the modulated conformation change of the fibrinogen on the OMe−PRX−PMB surface.[6] We believe that detailed studies of the effects of the number of α-CDs, methylation degree, and position of the functional groups on the fibrinogen adsorption will provide more information about the polymer−protein interaction, especially how the dynamic polyrotaxane surfaces influence the conformation of the adsorbed fibrinogens.

It should be noted that to fundamentally understand the essential structure of the polymers, it is also important to clarify the bulk structure of the polymer which directly affect its surface structure. Therefore, in order to get a general understanding of the polymer structure and its physical properties including the biocompatibility and protein adsorption, it is highly desired to clarify both bulk and surface structures of the polymer at a molecular level with combination of different techniques.

4. CONCLUSIONS

The surface reorganization behavior of various biomedical polymers including polyrotaxanes and random copolymers both in air and in water have been investigated by SFG vibrational spectroscopy on a molecular level. The four polymers were found to have similar side chain structures in air, but they show very different surface structures in water. Especially, the polyrotaxane threaded by methylated α-CDs shows a unique surface reorganization behavior in water, which is attributed to the hydrophobic interaction between the methoxy groups on the methylated α-CD molecules and methyl groups on the BMA side chains. It is believed that such an interaction can form some ordered structures at the OMe−PRX−PMB/water interface, which is further maximized by the surface mobility of the methylated α-CDs. The orientation analysis based on the SFG signals of the amide bands revealed that the fibrinogen

DOI: 10.1021/acsami.5b07760
ACS Appl. Mater. Interfaces 2015, 7, 22709−22718

adsorbed on the OMe−PRX−PMB surface exhibits a different conformation in comparison to those on the other polymer surfaces.

■ ASSOCIATED CONTENT

Supporting Information

The Supporting Information is available free of charge on the ACS Publications website at DOI: 10.1021/acsami.5b07760.

SFG spectra of polymer/PBS interfaces, SFG spectra of the C═O (*sps*-polarized), C−H, N−H, and O−H stretching regions of the polymer/fibrinogen solution interfaces, possible structures of the adsorbed fibrinogen on the polymer surfaces, and an orientation analysis of the fibrinogen (PDF)

■ AUTHOR INFORMATION

Corresponding Author

*E-mail: ye@cat.hokudai.ac.jp.

Present Address

§A.G.: Department of Chemistry, Emory University, Atlanta, GA 30322.

Notes

The authors declare no competing financial interest.

■ ACKNOWLEDGMENTS

This study was supported by a Grant-in-Aid for Scientific Research on Innovative Areas "Coordination Program" 759 (Grant 24108701) and a Grant-in-Aid for Scientific Research (B) Grant 23350058 from the Ministry of Education, Culture, Sports, Science & Technology (MEXT), Japan. N. Y. acknowledges a Grant-in-Aid for Scientific Research (B) Grant 25282142 from MEXT, Japan. The authors thank Prof. Zhan Chen from the University of Michigan for stimulating discussion on the calculation for the fibrinogen adsorption.

■ REFERENCES

(1) Chen, H.; Yuan, L.; Song, W.; Wu, Z.; Li, D. Biocompatible Polymer Materials: Role of Protein−Surface Interactions. *Prog. Polym. Sci.* **2008**, *33*, 1059−1087.

(2) Aizawa, Y.; Owen, S. C.; Shoichet, M. S. Polymers Used to Influence Cell Fate in 3D Geometry: New Trends. *Prog. Polym. Sci.* **2012**, *37*, 645−658.

(3) Seo, J.-H.; Yui, N. The Effect of Molecular Mobility of Supramolecular Polymer Surfaces on Fibroblast Adhesion. *Biomaterials* **2013**, *34*, 55−63.

(4) Harada, A.; Hashidzume, A.; Yamaguchi, H.; Takashima, Y. Polymeric Rotaxanes. *Chem. Rev.* **2009**, *109*, 5974−6023.

(5) Yui, N.; Katoono, R.; Yamashita, A. Functional Cyclodextrin Polyrotaxanes for Drug Delivery. *Adv. Polym. Sci.* **2009**, *222*, 55−77.

(6) Seo, J.-H.; Kakinoki, S.; Inoue, Y.; Yamaoka, T.; Ishihara, K.; Yui, N. Designing Dynamic Surfaces for Regulation of Biological Responses. *Soft Matter* **2012**, *8*, 5477−5485.

(7) Seo, J.-H.; Kakinoki, S.; Inoue, Y.; Nam, K.; Yamaoka, T.; Ishihara, K.; Kishida, A.; Yui, N. The Significance of Hydrated Surface Molecular Mobility in the Control of the Morphology of Adhering Fibroblasts. *Biomaterials* **2013**, *34*, 3206−3214.

(8) Seo, J.-H.; Kakinoki, S.; Inoue, Y.; Yamaoka, T.; Ishihara, K.; Yui, N. Inducing Rapid Cellular Response on RGD-Binding Threaded Macromolecular Surfaces. *J. Am. Chem. Soc.* **2013**, *135*, 5513−5516.

(9) Seo, J.-H.; Kakinoki, S.; Yamaoka, T.; Yui, N. Directing Stem Cell Differentiation by Changing the Molecular Mobility of Supramolecular Surfaces. *Adv. Healthcare Mater.* **2015**, *4*, 215−222.

(10) Herrick, S.; Blanc-Brude, O.; Gray, A.; Laurent, G. Fibrinogen. *Int. J. Biochem. Cell Biol.* **1999**, *31*, 741−746.

(11) Mosesson, M. Fibrinogen and Fibrin Structure and Functions. *J. Thromb. Haemostasis* **2005**, *3*, 1894−1904.

(12) Tsai, W. B.; Grunkemeier, J. M.; Horbett, T. A. Variations in the Ability of Adsorbed Fibrinogen to Mediate Platelet Adhesion to Polystyrene-Based Materials: A Multivariate Statistical Analysis of Antibody Binding to the Platelet Binding Sites of Fibrinogen. *J. Biomed. Mater. Res.* **2003**, *67*, 1255−1268.

(13) Wu, Y.; Simonovsky, F. I.; Ratner, B. D.; Horbett, T. A. The Role of Adsorbed Fibrinogen in Platelet Adhesion to Polyurethane Surfaces: A Comparison of Surface Hydrophobicity, Protein Adsorption, Monoclonal Antibody Binding, and Platelet Adhesion. *J. Biomed. Mater. Res., Part A* **2005**, *74*, 722−738.

(14) Chen, Z.; Shen, Y.; Somorjai, G. A. Studies of Polymer Surfaces by Sum Frequency Generation Vibrational Spectroscopy. *Annu. Rev. Phys. Chem.* **2002**, *53*, 437−465.

(15) Zhang, C.; Myers, J. N.; Chen, Z. Elucidation of Molecular Structures at Buried Polymer Interfaces and Biological Interfaces Using Sum Frequency Generation Vibrational Spectroscopy. *Soft Matter* **2013**, *9*, 4738−4761.

(16) Hankett, J. M.; Liu, Y.; Zhang, X.; Zhang, C.; Chen, Z. Molecular Level Studies of Polymer Behaviors at the Water Interface Using Sum Frequency Generation Vibrational Spectroscopy. *J. Polym. Sci., Part B: Polym. Phys.* **2013**, *51*, 311−328.

(17) Ye, S.; Tong, Y.; Ge, A.; Qiao, L.; Davies, P. B. Interfacial Structure of Soft Matter Probed by SFG Spectroscopy. *Chem. Rec.* **2014**, *14*, 791−805.

(18) Shen, Y. R. *The Principles of Nonlinear Optics*; Wiley-Interscience: New York, 1984.

(19) Zhang, D.; Ward, R. S.; Shen, Y. R.; Somorjai, G. A. Environment-Induced Surface Structural Changes of A Polymer: An in situ IR Plus Visible Sum-Frequency Spectroscopic Study. *J. Phys. Chem. B* **1997**, *101*, 9060−9064.

(20) Chen, Q.; Zhang, D.; Somorjai, G.; Bertozzi, C. R. Probing the Surface Structural Rearrangement of Hydrogels by Sum-Frequency Generation Spectroscopy. *J. Am. Chem. Soc.* **1999**, *121*, 446−447.

(21) Wang, J.; Woodcock, S. E.; Buck, S. M.; Chen, C.; Chen, Z. Different Surface-Restructuring Behaviors of Poly (Methacrylate)s Detected by SFG in Water. *J. Am. Chem. Soc.* **2001**, *123*, 9470−9471.

(22) Wang, J.; Paszti, Z.; Even, M. A.; Chen, Z. Measuring Polymer Surface Ordering Differences in Air and Water by Sum Frequency Generation Vibrational Spectroscopy. *J. Am. Chem. Soc.* **2002**, *124*, 7016−7023.

(23) Horinouchi, A.; Atarashi, H.; Fujii, Y.; Tanaka, K. Dynamics of Water-Induced Surface Reorganization in Poly(Methyl Methacrylate) Films. *Macromolecules* **2012**, *45*, 4638−4642.

(24) Shundo, A.; Hori, K.; Ikeda, T.; Kimizuka, N.; Tanaka, K. Design of a Dynamic Polymer Interface for Chiral Discrimination. *J. Am. Chem. Soc.* **2013**, *135*, 10282−10285.

(25) Gautam, K.; Schwab, A.; Dhinojwala, A.; Zhang, D.; Dougal, S.; Yeganeh, M. Molecular Structure of Polystyrene at Air/Polymer and Solid/Polymer Interfaces. *Phys. Rev. Lett.* **2000**, *85*, 3854−3857.

(26) Rangwalla, H.; Schwab, A. D.; Yurdumakan, B.; Yablon, D. G.; Yeganeh, M. S.; Dhinojwala, A. Molecular Structure of an Alkyl-Side-Chain Polymer-Water Interface: Origins of Contact Angle Hysteresis. *Langmuir* **2004**, *20*, 8625−8633.

(27) Wang, J.; Chen, X.; Clarke, M. L.; Chen, Z. Vibrational Spectroscopic Studies on Fibrinogen Adsorption at Polystyrene/Protein Solution Interfaces: Hydrophobic Side Chain and Secondary Structure Changes. *J. Phys. Chem. B* **2006**, *110*, 5017−5024.

(28) Weidner, T.; Breen, N. F.; Li, K.; Drobny, G. P.; Castner, D. G. Sum Frequency Generation and Solid-State NMR Study of the Structure, Orientation, and Dynamics of Polystyrene-Adsorbed Peptides. *Proc. Natl. Acad. Sci. U. S. A.* **2010**, *107*, 13288−13293.

(29) Yan, E. C. Y.; Fu, L.; Wang, Z.; Liu, W. Biological Macromolecules at Interfaces Probed by Chiral Vibrational Sum Frequency Generation Spectroscopy. *Chem. Rev.* **2014**, *114*, 8471−8498.

DOI: 10.1021/acsami.5b07760
ACS Appl. Mater. Interfaces 2015, 7, 22709−22718

(30) Li, G. F.; Ye, S.; Morita, S.; Nishida, T.; Osawa, M. Hydrogen Bonding on the Surface of Poly(2-Methoxyethyl Acrylate). *J. Am. Chem. Soc.* **2004**, *126*, 12198−12199.
(31) Ge, A.; Wu, H.; Darwish, T. A.; James, M.; Osawa, M.; Ye, S. Structure and Lateral Interaction in Mixed Monolayers of Dioctadecyldimethylammonium Chloride (DOAC) and Stearyl Alcohol. *Langmuir* **2013**, *29*, 5407−5417.
(32) Ge, A.; Peng, Q.; Wu, H.; Liu, H.; Tong, Y.; Nishida, T.; Yoshida, N.; Suzuki, K.; Sakai, T.; Osawa, M.; Ye, S. Effect of Functional Group on the Monolayer Structures of Biodegradable Quaternary Ammonium Surfactants. *Langmuir* **2013**, *29*, 14411−14420.
(33) Ge, A.; Peng, Q.; Qiao, L.; Yepuri, N. R.; Darwish, T. A.; Matsusaki, M.; Akashi, M.; Ye, S. Molecular Orientation of Organic Thin Films on Dielectric Solid Substrates: A Phase-Sensitive Vibrational SFG Study. *Phys. Chem. Chem. Phys.* **2015**, *17*, 18072−18078.
(34) Ye, S.; Noda, H.; Morita, S.; Uosaki, K.; Osawa, M. Surface Molecular Structures of Langmuir-Blodgett Films of Stearic Acid on Solid Substrates Studied by Sum Frequency Generation Spectroscopy. *Langmuir* **2003**, *19*, 2238−2242.
(35) Ye, S.; Noda, H.; Nishida, T.; Morita, S.; Osawa, M. Cd^{2+}-Induced Interfacial Structural Changes of Langmuir-Blodgett Films of Stearic Acid on Solid Substrates: A Sum Frequency Generation Study. *Langmuir* **2004**, *20* (2), 357−365.
(36) Tong, Y.; Zhao, Y.; Li, N.; Osawa, M.; Davies, P. B.; Ye, S. Interference Effects in the Sum Frequency Generation Spectra of Thin Organic Films. I. Theoretical Modeling and Simulation. *J. Chem. Phys.* **2010**, *133*, 034704.
(37) Tong, Y.; Zhao, Y.; Li, N.; Ma, Y.; Osawa, M.; Davies, P. B.; Ye, S. Interference Effects in the Sum Frequency Generation Spectra of Thin Organic Films. II: Applications to Different Thin-Film Systems. *J. Chem. Phys.* **2010**, *133*, 034705.
(38) Zhuang, X.; Miranda, P.; Kim, D.; Shen, Y. Mapping Molecular Orientation and Conformation at Interfaces by Surface Nonlinear Optics. *Phys. Rev. B: Condens. Matter Mater. Phys.* **1999**, *59*, 12632.
(39) Hirose, C.; Akamatsu, N.; Domen, K. Formulas For The Analysis of Surface Sum Frequency Generation Spectrum by CH Stretching Modes of Methyl and Methylene Groups. *J. Chem. Phys.* **1992**, *96*, 997.
(40) Tong, Y.; Li, N.; Liu, H.; Ge, A.; Osawa, M.; Ye, S. Mechanistic Studies by Sum Frequency Generation Spectroscopy: Hydrolysis of a Supported Phospholipid Bilayer by Phospholipase A_2. *Angew. Chem.* **2010**, *122*, 2369−2373.
(41) Ye, S.; Morita, S.; Li, G.; Noda, H.; Tanaka, M.; Uosaki, K.; Osawa, M. Structural Changes in Poly (2-Methoxyethyl Acrylate) Thin Films Induced by Absorption of Bisphenol A. An Infrared and Sum Frequency Generation (SFG) Study. *Macromolecules* **2003**, *36*, 5694−5703.
(42) Scatena, L. F.; Brown, M. G.; Richmond, G. L. Water At Hydrophobic Surfaces: Weak Hydrogen Bonding and Strong Orientation Effects. *Science* **2001**, *292*, 908−912.
(43) Tyrode, E.; Johnson, C. M.; Kumpulainen, A.; Rutland, M. W.; Claesson, P. M. Hydration State of Nonionic Surfactant Monolayers at the Liquid/Vapor Interface: Structure Determination by Vibrational Sum Frequency Spectroscopy. *J. Am. Chem. Soc.* **2005**, *127*, 16848−16859.
(44) Mondal, J. A.; Nihonyanagi, S.; Yamaguchi, S.; Tahara, T. Three Distinct Water Structures at a Zwitterionic Lipid/Water Interface Revealed by Heterodyne-Detected Vibrational Sum Frequency Generation. *J. Am. Chem. Soc.* **2012**, *134*, 7842−7850.
(45) Futamura, K.; Matsuno, R.; Konno, T.; Takai, M.; Ishihara, K. Rapid Development of Hydrophilicity and Protein Adsorption Resistance by Polymer Surfaces Bearing Phosphorylcholine and Naphthalene Groups. *Langmuir* **2008**, *24*, 10340−10344.
(46) Yaseen, M.; Zhao, X.; Freund, A.; Seifalian, A. M.; Lu, J. R. Surface Structural Conformations of Fibrinogen Polypeptides for Improved Biocompatibility. *Biomaterials* **2010**, *31*, 3781−3792.
(47) Wang, J.; Lee, S.-H.; Chen, Z. Quantifying the Ordering of Adsorbed Proteins in situ. *J. Phys. Chem. B* **2008**, *112*, 2281−2290.
(48) Jung, S. Y.; Lim, S. M.; Albertorio, F.; Kim, G.; Gurau, M. C.; Yang, R. D.; Holden, M. A.; Cremer, P. S. The Vroman Effect: A Molecular Level Description of Fibrinogen Displacement. *J. Am. Chem. Soc.* **2003**, *125*, 12782−12786.
(49) Chen, X.; Wang, J.; Boughton, A. P.; Kristalyn, C. B.; Chen, Z. Multiple Orientation of Melittin Inside A Single Lipid Bilayer Determined by Combined Vibrational Spectroscopic Studies. *J. Am. Chem. Soc.* **2007**, *129*, 1420−1427.
(50) Nguyen, K. T.; Le Clair, S. V.; Ye, S.; Chen, Z. Orientation Determination of Protein Helical Secondary Structures Using Linear and Nonlinear Vibrational Spectroscopy. *J. Phys. Chem. B* **2009**, *113*, 12169−12180.
(51) Sit, P. S.; Marchant, R. E. Surface-Dependent Conformations of Human Fibrinogen Observed by Atomic Force Microscopy under Aqueous Conditions. *Thromb. Haemost.* **1999**, *82*, 1053−1060.
(52) Agnihotri, A.; Siedlecki, C. A. Time-Dependent Conformational Changes in Fibrinogen Measured by Atomic Force Microscopy. *Langmuir* **2004**, *20*, 8846−8852.

DOI: 10.1021/acsami.5b07760
ACS Appl. Mater. Interfaces 2015, 7, 22709−22718